HHS Public Access

Author manuscript

Cell Microbiol. Author manuscript; available in PMC 2016 December 01.

Published in final edited form as:

Cell Microbiol. 2015 December ; 17(12): 1883–1899. doi:10.1111/cmi.12479.

Diverse Functional Outcomes of *Plasmodium falciparum* Ligation of EPCR: Potential Implications for Malarial Pathogenesis

Mark R. Gillrie[1], **Marion Avril**[2], **Andrew J. Brazier**[2], **Shevaun P. Davis**[1], **Monique F. Stins**[3], **Joseph D. Smith**[2,4], and **May Ho**[1]

[1]Department of Microbiology, Immunology and Infectious Diseases, University of Calgary, Calgary, Alberta, Canada T2N 4N1

[2]Center for Infectious Disease Research, Seattle, WA 98109, USA

[3]Department of Molecular Immunology and Microbiology, Johns Hopkins University, Baltimore, MD 21205, USA

[4]Department of Global Health, University of Washington, Seattle, WA 98109, USA

Summary

P. falciparum-infected erythrocytes (IRBC) expressing the domain cassettes (DC) 8 and 13 of the cytoadherent ligand PfEMP1 adhere to the endothelial protein C receptor (EPCR). By interfering with EPCR anti-coagulant and pro-endothelial barrier functions, IRBC adhesion could promote coagulation and vascular permeability that contribute to the pathogenesis of cerebral malaria. In this study, we examined adhesion of DC8- and DC13-expressing parasite lines to endothelial cells from different microvasculature, and the consequences of EPCR engagement on endothelial cell function. We found that IRBC from IT4var19 (DC8) and IT4var07 (DC13) parasite lines adhered to human brain, lung, and dermal endothelial cells under shear stress. However, the relative contribution of EPCR to parasite cytoadherence on the different types of endothelial cell varied. We also observed divergent functional outcomes for DC8 CIDRα1.1 and DC13 CIDRα1.4 domains. IT4var07 CIDRα1.4 inhibited generation of activated protein C (APC) on lung and dermal endothelial cells and blocked the APC-EPCR binding interaction on brain endothelial cells. IT4var19 CIDRα1.1 inhibited thrombin-induced endothelial barrier dysfunction in lung endothelial cells, while IT4var07 CIDRα1.4- inhibited the protective effect of APC on thrombin-induced permeability. Overall, these findings reveal a much greater complexity of how CIDRα1-expressing parasites may modulate malaria pathogenesis through EPCR adhesion.

Introduction

The adhesion of *Plasmodium falciparum*-infected erythrocytes (IRBC) to microvascular endothelium has long been recognized as a major pathological process of human malaria (White *et al*., 2013). Considerable evidence has accumulated to demonstrate that the process

For correspondence: May Ho, MD, Department of Microbiology, Immunology and Infectious Diseases, 3330 Hospital Dr. NW, Calgary, Alberta, Canada T2N 4N1. Tel: 403-220-8516; Fax: 403-210-8862; mho@ucalgary.ca.

occurs through the interaction between the parasite ligand *Plasmodium falciparum* erythrocyte membrane protein-1 (PfEMP1) and endothelial cell receptors (Rowe *et al.*, 2009). Cerebral malaria is a life-threatening complication associated with massive sequestration of IRBC in the cerebral microvasculature (MacPherson *et al.*, 1985). Parasites expressing PfEMP1 variants encoding domain cassettes (DC) 8 and 13 have been shown to bind to primary human brain endothelial cells (Avril *et al.*, 2012; Claessens *et al.*, 2012) and have been associated with severe malaria infections in children (Lavstsen *et al.*, 2012).

PfEMP1 proteins contain multiple Duffy binding like (DBL) and cysteine-rich interdomain region (CIDR) domains, which have been classified into different subtypes. The DC8 cassette consists of a specific combination of 4 domains (DBLα2-CIDRα1.1-DBLβ12-DBLγ4/6) and DC13 cassette consists of 2 domains (DBLα1.7-CIDRα1.4) (Rask *et al.*, 2010). A large scale screen of human plasma membrane proteins determined that DC8 and DC13 PfEMP1 bind to endothelial protein C receptor (EPCR) via CIDRα1.1 and CIDRα1.4 respectively (Turner *et al.*, 2013). More recent studies have revealed a total of six EPCR-binding subclasses (CIDRα1.1 and CIDRα1.4–1.8 domains) with only limited sequence identity among the variants (Lau *et al.*, 2015). In contrast, the majority of PfEMP1 variants encode CD36 binding activity in the corresponding CIDRα2–6 domains (Robinson *et al.*, 2003). EPCR plays a key role in regulating coagulation, inflammation, and vascular permeability (Mosnier *et al.*, 2007). Furthermore, because DC8/13 expressing parasites have broad endothelial tropism (Avril *et al.*, 2013) and EPCR has been demonstrated on endothelium of other vital organs such as the lung (Laszik *et al.*, 1997), EPCR may play a similar role as CD36 in mediating parasite cytoadherence in diverse anatomical locations.

EPCR is related to the major histocompatibility complex (MHC) class 1/CD1d family of molecules (Mosnier *et al.*, 2007). To date no specific signaling capabilities have been ascribed directly to EPCR, similar to other CD1d molecules that require associated signaling partners. Instead, EPCR is a receptor for the serum factor protein C and promotes its conversion to activated protein C (APC) by the thrombin-thrombomodulin complex. APC mediates its anticoagulant effect by inactivating the clotting factors Va and VIIa thereby diminishing thrombin generation. In addition, APC bound to EPCR on the endothelial cell surface elicits anti-inflammatory, anti-apoptotic, and pro-endothelial barrier responses by activating protease-activated receptor-1 (PAR-1). Conversely, thrombin is a pro-coagulant protease that converts soluble fibrinogen into fibrin and induces inflammatory responses and endothelial barrier permeability through PAR-1/PAR-3 activation (McLaughlin *et al.*, 2007). Although APC and thrombin elicit opposing responses, APC can alter thrombin signaling in endothelial cells and protect against endothelial barrier dysfunction induced by thrombin (Bae *et al.*, 2007).

The identification of EPCR as a receptor for DC8 and DC13 PfEMP1 has potential implications for the pathogenesis of severe malaria. IRBC induce tissue factor (TF) expression on endothelial cells in vitro, and TF expression is observed in brain sections from children who died from cerebral malaria (Francischetti *et al.*, 2007). The upregulation of TF may result in increased localized thrombin production. In addition, from pediatric autopsies EPCR surface expression is reduced and there are increased fibrin deposits at sites of IRBC sequestration in cerebral microvessels, suggesting there may be causal links between IRBC

cytoadherence and thrombin-dependent coagulation pathways (Moxon *et al.*, 2013). Lastly, interactions between recombinant CIDRα1.1/CIDRα1.4 and EPCR overlap with the PC/APC binding site (Turner *et al.*, 2013; Lau *et al.*, 2015), suggesting the potential for CIDR binding to impede APC activation and signaling leading to the coagulopathy and endothelial dysfunction seen in severe malaria.

To validate this disease model, several critical questions regarding IRBC-EPCR interactions remain. Although EPCR is highly expressed in arteries and veins, it is present in lower levels in many microvascular beds (Laszik *et al.*, 1997). It has not been determined if EPCR is sufficient to support IRBC adhesion to different primary human endothelial cells under shear stress, and it is unknown if IRBC impedes EPCR function on endothelial cells or modulates thrombin-induced barrier dysfunction similar to native EPCR ligands (Bae *et al.*, 2997). In order to understand the role and functional consequences of IRBC adhesion to EPCR on endothelial cells, we investigated the adhesion of EPCR-binding parasite lines to immortalized and primary human microvascular endothelial cells from brain, lung, and dermal sites. In addition, the effects of EPCR ligation by CIDR domains on APC generation/binding and barrier function of the various endothelial cell types were determined.

Results

PfEMP1 expression of parasite lines studied

To investigate the role of EPCR in parasite adhesion in different microvascular beds, two EPCR binding parasite lines were employed. The IT4var19 parasite line expressing a DC8 PfEMP1 (Avril *et al.*, 2012) and IT4var07 parasite line expressing a DC13 PfEMP1 (Avril *et al.*, 2013), were produced by repeated selection of the parental strain IT4 on brain and lung endothelial cells, respectively, followed by limited dilution cloning. As a control, a CD36-binding IT4var01 parasite line and recombinant protein from IT4var14 were used (Smith JD *et al.*, 1998). The schematic of the extracellular domain architecture and the corresponding domain cassette of the DC8 and DC13 PfEMP1 variants are shown in Figure S1A. IT4var07 CIDRα1.4 is 42.2% homologous to var19 CIDRα1.1 at the amino acid level. The expression of PfEMP1 in IT4var19 and IT4var07 clonal lines was monitored by flow cytometry using polyclonal antibodies specific to IT4var 19 DBLα2 (Figure S1C) and IT4var07 DBLα1.7 (Figure S1B), and by *var* transcription profiling (IT4var01) (Janes *et al.*, 2011).

Expression of EPCR on microvascular endothelial cells

EPCR is highly expressed on vascular endothelium lining large blood vessels, such as the aorta, inferior vena cava and human umbilical vein, but its expression is considerably lower on microvascular endothelium (Laszik *et al.*, 1997). For this study, we used transformed human brain microvascular endothelial cells (THBMEC) (Stins *et al.*, 2001) and primary human microvascular endothelial cells from brain (HBMEC), lung (HLMEC), and dermis (HDMEC). To investigate EPCR surface levels, we performed flow cytometric analysis of cells stained with the anti-EPCR mAb (clone RCR-252) that inhibits the binding of activated protein C to EPCR (Figure 1A). The results showed that EPCR was expressed on all three types of microvascular endothelium, but at a lower level than on the large vein-derived

human umbilical vein endothelial cells (HUVEC). Whereas EPCR expression on HUVEC was reduced by pre-incubation with TNF-α at 10 ng/ml for 16–20 h as previously reported (Menschikowski *et al.*, 2009), the effect varied on microvascular endothelial cells (Figure S2). EPCR expression was decreased by TNF-α activation of primary human brain endothelial cells, but its expression did not change on lung or dermal endothelial cells.

IT4var19 and IT4var 07 adhesion to THBMEC but not HBMEC was partially dependent on EPCR

We began by examining the adhesion of the parasite lines IT4var19 and IT4var07 on THBMEC in a parallel flow chamber assay as previously described (Yipp *et al.*, 2000). These parasite lines have been shown to bind avidly to different types of endothelial cells (Avril *et al.*, 2012) and immobilized recombinant EPCR protein (Turner *et al.*, 2013) in static binding assays. An IRBC suspension at 1% hematocrit and 4–5% parasitemia was withdrawn at 1 dyne/cm^2 over THBMEC monolayers. Adhesion of IRBC from both IT4var19 and IT4var07 parasite lines to transformed human brain microvascular endothelial cells (THBMEC) was observed in real time, and was inhibited by 29 and 33% respectively by an anti-EPCR antibody (40 μg/ml), suggesting that EPCR contributes to the overall adhesion to THBMEC under shear stress (Figure 1B and C).

As receptor expression may be modified in an immortalized cell line, the adhesion of IT4var19 and IT4var07 parasite lines was also examined on primary human brain endothelial cells (HBMEC). While IT4var19 adhesion was comparable between HBMEC and THBMEC, IT4var07 adhered to THBMEC, but had limited or no adhesion to primary brain endothelial cells (Figure 1D). In addition, anti-EPCR antibodies partially inhibited IT4var19-IRBC adhesion to THBMEC, but had limited effect on HBMEC. The lack of effect of antibody blockade on IT4var19 adhesion to primary brain endothelial cells was confirmed by siRNA knock down of EPCR protein expression by >80% as determined by Western blot (Figure 1E and Figure S3A). Therefore, there was variability between transformed and primary human brain endothelial cells in parasite adhesion and the DC8 and DC13-expressing parasite lines differed in their dependence on EPCR for binding to brain endothelial cells.

IT4var19 and IT4var07 adhesion to HLMEC was partially dependent on EPCR

In addition to cerebral sequestration, large numbers of malaria parasites are also seen in pulmonary alveolar capillaries in children with CM in Africa (Milner *et al.*, 2013), where sequestration is associated with pulmonary edema and microthrombi in 40% of cases (Milner *et al.*, 2014). Indeed, based on numerous autopsy studies from Malawi, a concept is emerging that severity of clinical disease in cerebral malaria correlates best with total sequestration in the body (Milner *et al.*, 2014), and the lung is one of the sites where it occurs. To determine if IT4var19 and IT4var07 expressing IRBC adhere to HLMEC under flow conditions, flow chamber assays were performed. As for brain endothelial cells, IRBC of IT4var19 adhered to HLMEC, and anti-EPCR inhibited adhesion by 38% (Figure 2A). Likewise, IT4var19-IRBC adhesion was decreased by 51% and 38% respectively for siRNA A and B knock down of EPCR protein expression compared to cells transfected with a negative control siRNA (Figure 2B and Figure S3B). Similar to IT4var19, adhesion of

IT4var07 was observed, and was inhibited to a mean of 33% by anti-EPCR (40 μg/ml) (Figure 2C).

IT4var19 and IT4var07 adhesion to HDMEC was not dependent on EPCR

Flow chamber experiments were also performed with IT4var19 and IT4var07 IRBC on dermal microvascular endothelial cells, an endothelium we have used extensively previously to study the interaction between IRBC and CD36, ICAM-1 and the $\alpha_5\beta_1$ integrin under shear conditions (Yipp *et al.*, 2000; Davis *et al.*, 2013). IRBC of IT4var19 bound robustly to HDMEC under flow conditions. However, unlike lung endothelial cells, IRBC adhesion was not reduced by anti-EPCR antibodies (Figure 3A) or siRNA knock down of EPCR protein expression (Figure 3B and Figure S3C), despite similar EPCR surface levels on HDMEC and HLMEC (Figure 1A). Furthermore, the adhesion was also not inhibited by anti-CD36 antibodies, suggesting cytoadherence of IT4var19 to HDMEC is mediated by as yet undetermined host molecule(s). The finding is consistent with recent evidence for other receptors that act in concert with EPCR to mediate IT4var19 binding to microvascular endothelial cells under static conditions (Avril *et al.*, 2013). Similar to IT4var19, the adhesion of IT4var07 to HDMEC also appeared to be EPCR-independent (Figure 3C). In contrast, adhesion of a CD36-binding variant IT4var01 to HDMEC was completely inhibited by anti-CD36 antibodies (Figure 3D).

CIDRα1.4 domain of IT4var07 inhibited endothelial APC generation

The above findings suggested that EPCR may have an accessory role in IRBC adhesion under flow conditions, and its participation in the adhesive interactions appears to depend on the type of endothelial cells at a particular vascular site. However, even if support of IRBC adhesion is not the primary role of EPCR, there may be functional consequences from a secondary interaction between EPCR and CIDRα1.1/CIDRα1.4 once binding has occurred through other receptor(s). The binding of protein C to EPCR is critical for both the generation of APC and subsequent cytoprotective and anti-coagulant functions of APC (Mosnier *et al.*, 2007). It has been suggested that since CIDRα1 protein binds to the same region of EPCR as protein C/APC and with similar affinity, EPCR binding by DC8- or DC13-expressing IRBC may contribute to a localized pro-coagulant phenotype in severe malaria by inhibiting APC generation or APC binding to EPCR (Turner *et al.*, 2013).

To investigate if ligation of EPCR on endothelial cells by the PfEMP1 CIDRα1.1 and CIDRα1.4 domains could lead to alterations in endothelial function, we coated 4.5 μm Dynal beads with recombinant CIDR proteins as previously reported (Avril *et al.*, 2013). Control beads were coated with the CD36-binding CIDRα5 domain from IT4var14 (Janes *et al.*, 2011). We first determined the effect of CIDRα1.1 and CIDRα1.4 on APC generation by an amidolytic APC generation assay using the chromogenic substrate CS-2166 (Sen *et al.*, 2007) with endothelial monolayers in the presence of CIDRα1.1-, CIDRα1.4- or control CD36-binding CIDRα5-beads. Consistent with reports in the literature that thrombomodulin expression is absent or minimal on human brain microvascular endothelial cells (Moxon *et al.*, 2013), we did not detect APC generation from protein C (PC) and thrombin in the presence of THBMEC or HBMEC (Figure S4A). In contrast, APC generation by HLMEC and HDMEC (approximately 1×10^5 cells/cm^2/400 μl) was equivalent to 4 nM and 3.5 nM

APC respectively as determined by an APC standard curve. More importantly, CIDRα1.4-beads inhibited APC generation by HLMEC and HDMEC to a similar extent as anti-EPCR antibody (20 μg/mL), whereas an isotype control rat IgG_1 (20 μg/ml) and CIDRα1.1- or CIDRα5-beads had no effect (Figure 4A and 4B).

CIDRα1.4 but not CIDRα1.1 protein inhibited binding of APC to EPCR

As we were unable to detect APC generation by either transformed or primary human brain endothelial cells, we investigated competition between APC and CIDR domains on brain endothelial cells using flow cytometry. In one format, CIDR and APC were co-incubated with THBMEC. Whereas APC binding was nearly completely abolished by CIDRα1.4 at 50 and 100 μg/ml, CIDRα1.1 and the negative control CIDRα5 had limited effect on APC binding (Figure 4C). To evaluate if var19CIDRα1.1 would inhibit APC binding if allowed to bind first, THBMEC were preincubated with recombinant CIDR proteins for 30 min prior to the addition of APC. Both CIDRα1.1 and CIDRα1.4 bound robustly to THBMEC but CIDRα5 did not (Figure 4D). In addition, the CIDRα1.4 had higher binding activity and reached a higher saturation binding level than CIDRα1.1. In agreement with the APC generation results in lung and dermal endothelial cells, only the CIDRα1.4 domain strongly and consistently inhibited APC binding to EPCR on brain endothelial cells (Figure 4E). Thus, our results showed differential inhibitory activity of CIDR domains on the APC-EPCR interaction on brain endothelial cells.

IT4var19 CIDRα1.1 domain inhibited thrombin-induced barrier dysfunction of lung but not brain endothelial cells through EPCR

A second endothelial cell function that may be regulated by EPCR is barrier function. The binding of the native ligand APC to EPCR has been shown to promote cytoprotective and pro-barrier effects in endothelial cells by altering thrombin signaling (Bae *et al.*, 2007). To determine if CIDRα1 domain ligation of EPCR could similarly modify thrombin-induced endothelial permeability, we next examined the effect of CIDRα1.1- and CIDRα1.4-beads on thrombin activity using a transwell assay (Gillrie *et al.*, 2007). Permeability at different time points was measured as trans-endothelial resistance (TER) using an EVOM voltohmmeter, with a drop in TER as an indicator of vascular leakage. We found that TER was reduced by both thrombin (5nM) and TNF-α (10ng/ml) but with different kinetics (Figure 5A). The effect of thrombin peaked at 30 min while that of TNF-α was seen at 12 h.

As with the APC generation assay, we were unable to induce a change in endothelial permeability with thrombin on immortalized endothelial cells (Figure S4B) that exhibited low baseline TER (≈30 ohms/cm^2), had reduced contact inhibition, and display weak and patchy staining of the junctional proteins VE-cadherin, claudin-5 and zona occludens-1 (ZO-1) (Figure S4C–E). Moreover, no drop in TER was observed with either thrombin (10 nM) or TFLLR-NH_2 (20μM), a synthetic ligand mimicking the tethered ligand produced by thrombin cleavage of PAR-1(Mihara *et al.*, 2013). In contrast, thrombin induced a 61 % drop in TER in primary brain endothelial cells, and the effect was not modified by pre-incubation of HBMEC with either CIDRα1.1- or CIDRα1.4-beads (Figure 5B).

Similar to HBMEC, thrombin induced a 43% drop in TER in lung endothelial cells (Figure 5C). However, pre-incubation of HLMEC with CIDRα1.1- but not CIDRα1.4- or CIDRα5 beads for 1h prior to the addition of thrombin resulted in a decrease in the maximal drop in TER from 43 to 17% (Figure 5C). This inhibitory effect was specific to thrombin as there was no effect of CIDRα1.1-beads on TNF-α-induced permeability (Figure 5D). Furthermore, the effect was partially reversed by EPCR blockade with anti-EPCR (20 μg/mL) (Figure 5E), or knock down of EPCR protein by siRNA (Figure 5F). In contrast to thrombin, CIDRα1.1-beads had no effect on barrier dysfunction in response to TFLLR-NH_2 (20μM) (Figure 5G), suggesting that the protease activity of thrombin is required for the EPCR-dependent barrier protective effect of CIDRα1.1 beads.

CIDRα1.4 domain of IT4var07 inhibited the barrier protective effect of APC in HBMEC and HLMEC

The strong competition between APC and CIDRα1.4 for binding to EPCR on THBMEC (Figure 3D and E) suggested that it might inhibit the protective effect of APC. In these experiments, HBMEC and HLMEC were pre-incubated for 8 min with CIDRα beads followed by 20–40 nM APC for an additional 30 min after which thrombin was added and TER measured. As expected, APC by itself protected HBMEC and HLMEC monolayers from thrombin-induced barrier dysfunction by 47% and 56% respectively (Figure 5H and I). The protective effect of APC in both cases was reversed by >90% by pre-incubation with CIDRα1.4- but not CIDRα1.1- or CIDRα5-coated beads.

Morphological changes in HLMEC induced by thrombin

The functional changes in permeability noted above were associated with significant morphological changes in the adherens junction protein ZO-1 and F-actin by immunofluorescence microscopy. Whereas control cells stained evenly for ZO-1 in cortical rings at sites of cell-cell junctions that colocalized with filamentous F-actin stained with rhodamine-labeled phalloidin (Figure 6A), cells incubated with thrombin displayed discontinuous staining for ZO-1 protein and considerable gap formation. Notably, the number of intercellular gaps/mm^2 (Figure 6B) and the number of breaks/cell in ZO-1 staining (Figure 6C) were partially reversed by pre-incubation with CIDRα1.1- but not CIDRα1.4-beads (Figure 6B and C). On the other hand, while APC reduced thrombin-induced disruption of ZO-1 staining and intercellular gaps formation by greater than 50%, this protective effect was lost in the presence of CIDRα1.4-beads (Figure 6B and C).

Intact IRBC from IT4var19 and IT4var 07 parasites did not inhibit thrombin-induced APC generation or endothelial permeability

To determine if the effects on thrombin-induced permeability and APC generation by CIDRα1.1 and CIDRα1.4-coated beads respectively are also mediated by intact IRBC expressing CIDRα1.1 and CIDRα1.4, we performed APC generation and transwell assays using IRBC containing late trophozoites purified on a MACS column (>95% purity) from the parasite lines IT4var19 and IT4var07. Neither parasite line modulated thrombin-induced permeability (Figure S5A and B) nor inhibited APC generation (Figure S5C and D). The lack of effect was not due to detachment of IRBC over the course of the experiments, as static binding assays with IRBC showed that IRBC adhesion was maintained for the

duration of the functional experiments, i.e 30 min for maximal thrombin activity (5 nM) on TER, and 2 h for the APC generation assay in which a lower dose of thrombin (2 nM) was used.

Discussion

Recent findings showing an increase of EPCR-binding parasites in pediatric patients with severe malaria (Turner *et al.*, 2013), coupled with the loss of EPCR expression and presence of fibrin deposits at sites of cerebral sequestration (Moxon *et al.*, 2013), suggested that there may be causal links between IRBC cytoadherence and coagulation pathways in the pathogenesis of cerebral malaria. However, the interaction of IRBC with EPCR under shear stress and the functional consequences of EPCR adhesion have not been specifically investigated. In this study, we examined the relative contribution of EPCR in parasite adhesion to different endothelial cell types under shear stress, and the effect of EPCR binding on APC generation/binding and endothelial barrier function.

We began by determining the role of EPCR in supporting the adhesion of two parasite lines IT4var19 and IT4var07 that have been shown to encode EPCR binding activity (Turner *et al.*, 2013) and have broad and avid endothelial binding activity under static conditions (Avril *et al.*, 2012). Since EPCR expression levels may differ on microvascular endothelium and other receptors may act in concert with EPCR to mediate firm adhesion, it is important to understand the relative contribution of EPCR to overall parasite binding activity in different vascular beds for designing anti-adhesive therapies. We found that both parasite lines bind to microvascular endothelial cells from brain, lung, and dermis in flow-based adhesion studies. However, the relative contribution of EPCR differed among the cell types. While EPCR blockade partially inhibited IRBC binding to THBMEC and HLMEC, it had no effect on binding to HBMEC and HDMEC, despite EPCR expression on all four cell types. These results strongly suggest that the adhesion of these parasite lines is largely dependent on the interaction of PfEMP1 domains other than CIDRα1.1 and CIDRα1.4 with as yet unidentified host receptors. The lack of a role for EPCR on the adhesion of these parasite lines on primary brain microvascular endothelium was unexpected, but the observation further highlights the heterogeneity of receptor usage by IRBC in different vascular beds, and possibly on primary versus transformed brain cells.

The above findings on IRBC binding to EPCR contrast with CD36 binding parasites, another parasite adhesion trait which has also been mapped to the first CIDR domain located in the PfEMP1 head structure. PfEMP1 proteins have diverged into CD36 binding (group B and C *var* genes containing CIDRα2–6) and EPCR binding variants (group A and B *var* genes containing CIDRα1) (Turner *et al.*, 2013; Lau *et al.*, 2015). Compared to the incremental contribution of the CIDRα1-EPCR interaction to overall binding, the CIDRα2–6-CD36 binding interaction is pivotal to IRBC adhesion in vascular beds where both ligand and receptor are expressed, so that interventions inhibiting this interaction completely abrogated IRBC adhesion under flow conditions both in vitro and in vivo (Ho *et al.*, 2000; Yipp *et al.*, 2003). Taken together, the findings would suggest that anti-adhesive therapy directed towards CIDRα1-EPCR interaction might be significantly less effective in reducing IRBC sequestration.

To directly assess the effect of EPCR mediated adhesion on APC generation and endothelial barrier function, we used beads coated with recombinant CIDRα1.1 and CIDRα1.4 proteins. We observed divergent functional outcomes for the two EPCR ligands. Whereas CIDRα1.4-beads inhibited APC generation to the same extent as anti-EPCR antibodies on lung and dermal endothelial cells, CIDRα1.1-beads had no effect. Moreover, CIDRα1.4 inhibited the protective effect of APC on thrombin-induced endothelial permeability on both brain and lung endothelial cells. The differential effect for the two CIDR proteins appeared to be at least in part due to competitive binding with APC by CIDRα1.4, as the recombinant protein inhibited binding of APC to THBMEC, but CIDRα1.1 did not. Direct measurement of the binding of recombinant CIDRα1.1 and CIDRα1.4 to transformed brain microvascular endothelial cells also indicated that CIDRα1.4 domain had much greater binding activity than CIDRα1.1 and reached a higher level of saturation binding. These results are in keeping with the lower EPCR-binding affinity for recombinant IT4var19 CIDRα.1.1 (K_D = 16nM) compared to IT4var07 CIDRα1.4 (K_D = 0.37nM) by surface plasmon resonance assays (Lau *et al.*, 2015).

In contrast to the inhibitory effects of CIDRα1.4-beads on APC generation and function, CIDRα1.1-beads ameliorated thrombin-induced barrier dysfunction on lung endothelial cells but had no effect on brain endothelial cells. The drop in TER induced by thrombin was partially reversed by CIDRα1.1-beads, as was the disruption of endothelial junctions. Actin stress fiber formation, however, was not affected, suggesting that the effect of CIDRα1.1-beads was mediated by a myelin light chain kinase/actin-independent pathway. In the context of severe malaria, this finding is significant because adherent IRBCs have been reported to up-regulate tissue factor expression on endothelial cells (Francischetti *et al.*, 2007) which may lead to excessive localized thrombin signaling and endothelial dysfunction. As CIDR domains did not directly affect endothelial barrier properties on their own, this suggests that the divergent functional properties may be under selection in part to modulate thrombin-induced proinflammatory signaling pathways at sites of IRBC sequestration.

The mechanism by which CIDRα1.1-beads modulated the effect of thrombin was not directly investigated. Thrombin induces endothelial barrier disruption through PAR-1/PAR-3 signaling via the G proteins $G_{\alpha q}$ and $G_{\alpha 13}$ (McLaughlin *et al.*, 2007), leading to actin stress fiber formation and transient cell retraction (Finigan *et al.*, 2005). APC binding to EPCR can alter thrombin signaling through PAR-1 by at least four proposed mechanisms that may not be mutually exclusive. First, thrombin cleavage of PAR-1 can be re-directed by APC, or mutant protease-deficient APC, such that thrombin no longer induces barrier disruption by cleaving PAR-1 at Arg-41 but rather by barrier protective cleavage at Arg-46 (Bae *et al.*, 2007). Alternatively, as a serine protease, EPCR-bound APC can also directly cleave PAR-1 at Arg-46 generating the same cytoprotective tethered ligand (Mosnier *et al.*, 2013) that in turn induces S1P1 signaling and barrier protection (Finigan *et al.*, 2005). Third, PAR-1 normally resides in both caveolin-rich and caveolin-poor lipid rafts in the cell membrane. On thrombin activation, PAR-1 is mobilized from the caveolin-rich compartment. EPCR engagement by APC may lead to the retention of PAR-1 within caveolin-rich lipid rafts to direct PAR-1 towards barrier protective signaling (Russo *et al.*,

2009). Finally, an alternate cytoprotective APC signaling pathway has also been proposed that occurs through the cleavage of PAR-3 at Arg 41, with the resulting PAR-3 tethered ligand presumably shifting PAR-1 from $G_{\alpha 13}$ to barrier protective signaling (Burnier and Mosnier, 2013). The results presented in this study are most in keeping with the first mechanism where engagement of EPCR by a protease-deficient ligand, in this case CIDRα1.1, can change thrombin/PAR-1 signaling from barrier disrupting to barrier protective. Moreever, the barrier protective activity of CIDRα1.1 is both specific to and requires the proteolytic activity of thrombin on PAR-1, as it had no effect on TNF-α-induced permeability, or the disruption of barrier function by TFLLR-NH2, the synthetic PAR-1 agonist that acts as the Arg-46 tethered ligand.

The functional data above are supported by our analysis of the CIDRα1.1 and CIDRα1.4 domains based on a combination of mutagenesis, inhibitory antibodies and competitive binding studies (Sampath S *et al.*, companion manuscript). The results show subtle differences in the binding footprints of a number of CIDRα1.1 and CIDRα1.4 domains on EPCR, resulting in distinct affinities and APC blockade activity. Although the newly resolved crystal structure of two recombinant CIDRα1.4 domains with EPCR show that the binding surfaces are conserved in shape and bonding potential despite extensive sequence diversity (Lau *et al.*, 2015), our results would suggest that the subtle differences between CIDRα1.1 and CIDRα1.4 engagement with cell surface expressed EPCR are sufficient to allow the two ligands to activate or inhibit distinct signaling pathways and hence elicit divergent functional outcomes.

The divergent effects of CIDRα1.1 and CIDRα1.4 we observed may have significant clinical relevance. Autopsy studies of pediatric patients who died of severe cerebral malaria have identified two histopathological groups (Taylor *et al.*, 2004; Milner *et al*, 2014; Dorovini-Zis *et al.*, 2011). The CM1 group (~25% of cases) is associated with IRBC sequestration alone and the CM2 group (~75% of cases) is associated with IRBC sequestration plus ring hemorrhages, fibrin deposition, and intravascular monocytes limited largely to the brain, kidney and lung (Milner *et al.*, 2014; Dorovini-Zis *et al.*, 2011). The molecular mechanisms contributing to these pathophysiologic differences have not been defined, but it is tempting to speculate that the CM1/CM2 dichotomy may be related to the divergent functional effects of CIDRα1.1 and CIDRα1.4 domains that we have shown here (Figure 7). In a recent report on differential PfEMP1 expression in the brain, gut and lung of patients with the two clinical CM types, Group A *var* genes (of which IT4var07 is a member) were most frequently seen in CM2 patients, while group B *var* genes (of which IT4var19 is an example) were highest in CM1 patients (Tembo *et al.*, 2014). It will be important to investigate if specific DC8 or DC13 CIDRs are associated with more virulent infections or have prognostic significance that could guide therapeutic interventions.

Our findings also suggest the possibility of organ specific differences in parasite-EPCR binding phenotypes. Although DC8-IRBC adhered to brain and lung endothelial cells, the CIDRα1.1 domain was only able to shift thrombin signaling from destructive to barrier protective pathways in lung endothelial cells. Coupled with the lack of thrombomodulin expression on brain microvascular endothelial cells, this may leave cerebral microvessels more dependent on systematically released APC. On the other hand, there may be specific

vascular niches such as the lung where the thrombin-modulating phenotype is manifested, possibly depending on the expression levels of regulatory factors in the coagulation pathway (e.g. EPCR, thrombomodulin, TF) and the milieu of pro-inflammatory cytokines and other endothelial stimuli present. It remains to be determined whether the functional divergence we observed could be extrapolated to the intact EPCR-binding IRBC, as IRBC adhesion did not alter APC generation or barrier function in our hands. IRBC are likely to have a lower ligand density on the cell surface compared to coated beads, so that a functional effect may be more difficult to detect. In addition, in vitro assays may not completely recapitulate the hemodynamics/adhesion molecule expression of a microvessel where the IRBC may be binding to EPCR and other adhesion molecules with higher avidity than on a one-dimensional monolayer.

In summary, we have performed functional studies on the interaction between *P. falciparum* and the newly defined receptor EPCR. We showed that EPCR on primary microvascular endothelium supported adhesion under shear stress of parasite lines expressing both DC8 and 13 that are associated with severe malaria in African children. However, the contribution of EPCR to the overall adhesion varied among endothelial cells from different vascular beds. These findings support a much more complex paradigm of interaction between parasite ligands and EPCR than the initial hypothesis that parasites bind EPCR in the cerebral circulation and vascular dysfunction ensues. Instead, some parasites, like IT4var19, may selectively bind to a region on EPCR that does not interfere with anti-coagulant function and at the same time subvert EPCR signaling function to minimize thrombin-induced barrier dysfunction during malaria infection. Other parasites, such as IT4var07, may contribute to pathogenesis by inhibiting the generation and/or binding of APC. Until an appropriate in vivo model for cerebral malaria is developed, the organ-specific and divergent functional effects of the two CIDR domains shown with recombinant protein-coated beads provides an important theoretical framework to guide future research concerning the complex role of EPCR in the pathogenesis of severe malaria.

Experimental procedures

Ethics Statement

Discarded human foreskins were collected for the isolation of endothelial cells for this study with written informed consent of the parents. Normal red blood cells were collected from adult volunteer donors with their written informed consent. Both protocols were reviewed and approved by the Conjoint Ethics Board of Alberta Health Services and The University of Calgary, Alberta, Canada.

Rabbit immunizations were carried out in strict accordance with the recommendations in the Guide for the Care and Use of Laboratory Animals of the National Institutes of Health. Rabbit immunizations were performed by custom vendor at Pocono Rabbit Farm and Laboratory under an approved protocol by the Institute Animal and Care Use Committee at Seattle Biomedical Research Institute (Protocol JS-ABP-04).

Tissue culture and other reagents

Unless otherwise specified, all tissue culture reagents were obtained from Invitrogen Life Technologies Canada Inc. (Burlington, ON) and chemical reagents were purchased from Sigma-Aldrich Co. (St. Louis, MO). The thrombin inhibitor recombinant hirudin and chromogenic substrate CS-2166 were purchased from Hyphen Biomed (Neuville-sur-Oise, France). Protein C and recombinant human activated protein C (rhAPC) were purchased from Enzyme Research Laboratories (South Bend, IN). Activated protein C (APC) used for the blocking binding assay was from Sigma. Recombinant human TNF-α was purchased from Becton Dickinson, Bedford, MA). Endothelial basal medium (EBM) and supplements were purchased from Lonza Group Ltd. (Walkersville, MD).

Antibodies

The following antibodies were used: anti-human EPCR clone RCR-252 (Sigma); anti-human CD36 clone FA6–152 (Beckman Coulter Canada, Inc., Mississauga, ON); goat anti-APC (GAPC-AP, Affinity Biologicals, Ancaster, ON); Alexa Fluor 488-labeled goat anti-rat IgG_1 (Becton Dickinson, San Diego, CA); Alexa Fluor 488-labeled chicken anti-goat (Molecular Probes); Alexa Fluor 488-labeled goat anti-rat IgG_1 (Becton Dickinson); and FITC-labeled goat anti-mouse IgG (Molecular Probes).

Parasites

The experiments were performed with the parasite lines IT4var19, IT4var07, and IT4var01, which were all isolated from the parental strain IT4/25/5 by limiting dilution cloning. (Avril *et al.*, 2013). The expression of PfEMP1 in the three parasite lines was monitored by flow cytometry with polyclonal antibodies and *var* gene transcription profiling (Janes et al., 2011). The parasites lines were expanded in 7–10 cycles and gelatin-floated, after which they were frozen in aliquots. For flow chamber assays, frozen aliquots of parasites were thawed and cultured for 24 to 30 h at 37°C and 95% N_2/5% CO_2 with RPMI plus 10% pooled human AB serum until the late trophozoite/early schizont stage as determined by light microscopy. Thawed parasites were used in experiments for up to 3–4 cycles after which they were discarded.

P. falciparum CIDR-coated Dynal beads

EPCR-binding CIDRα1.1- and CIDRα1.4-beads, CD36-binding CIDRα5-beads, and non-binding DBLα0.23-beads were prepared as previously described [12]. In brief, His_6-MBP-TEV-PfEMP1 insert-StrepII constructs containing recombinant IT4var19 CIDRα1.1 (C485-C732), IT4var07 CIDRα1.4 (P467-C717), IT4var14 CIDRα5 (W486-E755) and IT4var14 NTS-DBLα0.23(M1-C484) proteins were produced using *E. coli* K12 (pSHuffle Express, New England Biolabs Inc., Ipswich, MA). Recombinant proteins were purified in a two-step procedure first by Ni-NTA (GE Healthcare Bio-Sciences, Pittsburgh, PA) followed by Strep-Tactin resins (Qiagen, GmBH, Hilden, Germany). Purified recombinant proteins were coated onto 10^7 sheep anti-mouse IgG coated Dynal beads (Invitrogen) with mouse anti-MBP monoclonal antibody.

Microvascular endothelial cells

Four types of microvascular endothelium were used in this study. Cultures from thawed cells were maintained in EBM with supplements provided by the manufacturer. THBMEC was a brain microvascular endothelial cell line derived from cells that were transfected with a pBR322 based plasmid containing simian virus 40 large T antigen (SV40-LT) (Stins et al., 2001). These cells were used in the selection of the EPCR binding parasite line IT4var19. Cells used in this study were from passage 38 to 42.

Primary human brain microvascular endothelial cells (HBMEC) isolated from normal cerebral cortex were purchased from Cell Systems (Kirkland, WA) at passage three. Cells were expanded and aliquots at passage five were cryopreserved until use. Cells were used until passage 10 after thawing. HBMEC were tested by the manufacturer for expression of von Williebrand factor, and were positive for acetyated low density lipoprotein uptake, and CD31 expression. All cells tested negative for mycoplasma and HIV.

Primary human lung microvascular endothelium (HLMEC) was purchased from Lonza. The cells were expanded and aliquots at passage four were cryopreserved. Cells were used until passage 10 after thawing. HLMEC were tested by the manufacturer for expression of von Williebrand factor, and were positive for acetyated low density lipoprotein uptake, and CD31 expression. All cells tested negative for mycoplasma and HIV. HLMEC were further characterized in our laboratory for VE-cadherin, ZO-1, ICAM-1 and CD36 expression (Gillrie et al., 2007).

Primary human dermal microvascular endothelial cells (HDMEC) were harvested from discarded neonatal human foreskins as described (Yipp et al., 2000). Harvested cells were seeded in 25 cm tissue culture flasks in supplemented endothelial basal medium (EBM) as for the lung cells. When cells were confluent, they were purified with CD31-coated beads in a MACS LS column (Miltenyi Biotec, Auburn, CA). Only cell preparations that were >95% positive for CD31 and CD36 expression by flow cytometry were maintained for experiments. Experiments were performed with cells from passages two to five that were demonstrated to consistently support IRBC adhesion.

Small interference RNA for *PROCR*

Knock down of *PROCR* (EPCR) mRNA in HLMEC and HDMEC was performed as previously described (Davis et al., 2013). Briefly, endothelial cells were transfected 24 h after seeding in 35 mm tissue culture dishes when the cells were 70 to 80% confluent. The transfection mixture of 10 μl HiPerfect (Qiagen) and 20nM siRNA ‘A’ (S100088130) or ‘B’ (S100088137) for PROCR or scrambled siRNA (All Stars Negative Control, S103650318) was added in 1.0 ml of Opti-MEM medium. Four hours after transfection, 1.0 ml of EBM was added to each dish. Monolayers were used for flow chamber studies 72 h after transfection. Cells or cell lysates collected at the same time confirmed gene knockdown of EPCR by 80–90% as determined by Western blot. For siRNA experiments on endothelial permeability, cells were sub-cultured into transwells 24 h post siRNA transfection and used in permeability experiments in 72 h.

Flow chamber assay

IRBC-endothelial cell interactions at fluid shear stresses approximating those in the microvasculature were studied using a parallel plate flow chamber as described (Yipp et al., 2000). A 1% IRBC suspension at 4–5% parasitemia was infused over confluent HLMEC or HDMEC monolayers at 1 dyne/cm^2 that allowed us to optimally visualize the adhesive interactions in real time. Experiments were recorded and analyzed off-line. For inhibition experiments, monolayers were pre-incubated with inhibitory or control antibodies at the indicated concentrations for 30 min at 37°C. An adherent IRBC was defined as one which remained attached for >10 sec. Results were expressed as the mean number of adherent IRBC/mm^2 in 4 randomly selected fields of view (20X) at the end of a 7-min infusion.

APC generation by endothelial cells

APC generation was determined by an amidolytic APC generation assay (Sen et al., 2007). Endothelial cells were seeded in 48-well plates with 300 μl EBM /well. Cells were grown until 1 day post-confluence. At the time of experimentation, cells were washed x 1 with PBS to remove any serum. The reaction buffer consisting of 1mM $MgCl_2$, 1mM $CaCl_2$, 20mM HEPES, 0.1% BSA at pH 7.4 was added at 300 μl/well for 30 min at 37°C to equilibrate. At time zero, 80nM protein C and 2nM human thrombin were added and incubated for 2 h at 37°C. To confirm that the APC generation was EPCR-dependent, HLMEC were preincubated with anti-EPCR or control rat IgG at 20 μg/ml for 30 min at 37°C. To determine if CIDRα1.1/1.4- or CIDRα5–beads could affect APC generation, monolayers were pre-incubated with coated beads (2.5×10^6/cm^2) for 1 h prior to the addition of protein C and thrombin. At the 2 h time point, 100 nM hirudin was added to all wells and incubated for 5 min to inhibit thrombin activity. After hirudin incubation, the chromogenic substrate S-2166 was added to a final concentration of 500 μM and samples of 50 μl from each well were collected at time 0 and at 5- min intervals thereafter for a total of 10 min. Samples were read immediately on a spectrophotometer at 405nm. Results were expressed as nM APC based on the APC standard curve generated using APC in wells without endothelial cells.

APC binding inhibition assay between CIDR recombinant protein and APC on a brain microvascular endothelial cell line

Cells from an immortalized human brain endothelial cell line (THBMEC) [20] were lifted with 10 mM EDTA, washed and resuspended in complete HBSS (HBSS with 3 mM CaCl2, 0.6 mM MgCl2, 1% bovine serum albumin) for 30 min at room temperature prior to the experiment to restore divalent cations (Liaw et al., 2001). In format 1, cells were first incubated with different concentrations of recombinant var19 CIDRα1.1, var07 CIDRα1.4 or var14 CIDRα5 domains for 30 min at 4°C, washed 2X with complete HBSS and then incubated with APC (50 μg/ml) for 30 min at 4 C. In format 2, cells were co-incubated with CIDR recombinant proteins and APC. After washes, binding of APC was detected with a goat anti-APC mAb (20 μg/ml), followed by a secondary chicken anti-goat Alexa 488-labeled antibodies (10 μg/ml). After final washes, cells were fixed with 4% w/v of paraformaldehyde for 10 min and antibody-labeled cells were analyzed by LSRII (Becton Dickinson). Single live cells were gated using the Live/Dead fixable violet Dead cell stain

kit (Molecular Probes). Data was analyzed by FlowJo 7.6.5 software (Tree Star Inc.). Results were expressed as percent of binding of APC (= proportion of cells antibody reactive x MFI of total cell population).

For titration of CIDR recombinant protein binding, THBMEC cells were lifted with 10 mM EDTA, washed and resuspended in 1X PBS with 0.5% BSA. Cells were then incubated with different concentrations of recombinant CIDR domains for 30 min at 4°C. After two washes with PBS-BSA, CIDR was detected by labeling with rabbit polyclonal anti-StrepII tag antibody (10 μg/ml, Genscript) for 30 min at 4°C, followed by goat anti-rabbit Alexa488 coupled antibodies, for 30 min at 4°C (4μg/ml, Molecular Probes). Flow cytometry was done as described above. Results were expressed as normalized MFI of the whole cell population.

Transwell permeability assay

Transendothelial resistance (TER), a measure of the resistance and hence integrity across the endothelial cell monolayer, was monitored using the EVOM-1voltohmeter with STX probe (World Precision Instruments, Sarasota, FL) as previously described (Gillrie et al., 2007). Briefly, endothelial cells were cultured in 12mm polyester transwells with 0.4 μm pores (Corning Life Sciences, Tewksbury, MA) until 48 to 72h post-confluence. 0.5 ml of EBM was added to the top well and 1.5 ml to the bottom well. One hour prior to experimentation, the medium in both wells was replaced with serum-free EBM.

For experiments to determine changes in permeability in response to thrombin (5 nM) or TNF-α (10ng/ml), 25 μl of medium from the top-well was replaced by the stimulating agent in PBS after baseline TER was measured. TER was determined at indicated intervals for a total of 24 h. Results were expressed as ohms x cm^2 after subtraction of background resistance of wells without cells (~100 ohms x cm^2).

To determine if CIDRα1.1-, CIDRα1.4- or CIDRα5–beads could affect the increase in endothelial permeability induced by thrombin or TNF-α, monolayers were pre-incubated with coated beads ($2.5\times10^6/cm^2$) for 1h prior to the addition of the mediators. To determine if the inhibitory effect of CIDRα1.1-beads on thrombin-induced permeability was EPCR-dependent, monolayers were pre-incubated with anti-EPCR or rat IgG (20 μg/ml) for 30 min prior to the addition of beads. As a positive control for cytoprotective EPCR signaling, 20nM APC was added 1 hour prior to stimulation with TNF-α or thrombin.

Transwell assay and APC generation with intact IRBC

Transwell and APC generation assays as described above were also performed with 2×10^6 IRBC of IT4var19, IT4var07 or uninfected erythrocytes (NRBC). IRBC were purified on a MACS LS column. IRBC at the trophozoite stage (>95% purity) were resuspended in serum-free EBM before adding to HLMEC monolayers to provide a single uniform layer.

Confocal immunofluorescence microscopy

Endothelial cells were seeded into μ-slide$VI^{0.4}$ (Ibidi GmbH, Munich, Germany) for experiments with CIDRα-coated bead (Davis et al., 2013), or gelatin-coated glass coverslips

for characterization of junctions as previously described (Gillrie et al., 2007). All experiments were done at 48- to 72-hour post-confluence with endothelial cells seeded at 5×10^4 cells/cm^2. Polyclonal anti-ZO-1 (1:250, Invitrogen), polyclonal anti-claudin-5 (1:50. Neo Markers, Fremont CA) and monoclonal anti-VE-Cadherin (2 μg/ml, clone F-8, Santa Cruz Biotech., Dallas, Texas) antibodies were used for characterization of endothelial cell junctions.

For CIDRα-coated bead experiments, beads were added to HLMEC in serum-free EBM. Beads were added at 2.5×10^6/cm^2 and were gently pipetted through the chamber 3 times before being allowed to settle for 30 min. APC (20nM) was added gently 30 min after bead addition for 30 min prior to thrombin. After stimulation with thrombin (5nM) for 30 min, Ibidi chambers were washed twice with warm HBSS, fixed with 1% PFA in HBSS, followed by blocking with BSA/PBS and incubation with primary antibody (ZO-1, 1:250) in blocking buffer overnight. Alexa-488-labeled secondary antibodies were added at 1:500 for an hour after which Hoechst 33342 (1μg/ml) or rhodamine phalloidin (1:60) (Molecular Probes / Life Technologies) were added. After washing, ibidi chambers containing PBS were imaged using an Olympus IX81 FV100 laser scanning confocal microscope with 40X OPlanFLN oil objective NA 1.30 (Olympus Canada Inc., Toronto Ont). Images were acquired at 640×640 pixels (158μmx158μm) and 20–30 0.5μm stacks at 2x Nyquist sampling using FV1000 acquisition software.

All image analysis was done using ImageJ v1.48 (NIH, Rockford Maryland). Gaps in HLMEC were quantified by randomly selecting 3 microscopic fields (40x) for each condition in each experiment. A gap was defined as a single area larger than 20 pixels in diameter devoid of actin staining. Results obtained from 3 independent experiments were expressed as gaps per mm^2. ZO-1 discontinuity was determined from the same set of images using ImageJ by manually counting and measuring the total number of gaps in ZO-1 staining at cell-cell junctions >15pixels divided by the total number of complete nuclei (cell count).

Statistical analysis

Statistical analysis was performed using GraphPad Prism (version 6, GraphPad Software Inc.). Data are expressed as mean ± SEM unless otherwise stated. All data was compare using ANOVA followed by post-hoc multiple comparisons using Tukey's test unless otherwise specified. P values of 0.05 or less were considered statistically significant and denoted as * for $p < 0.05$, ** for $p < 0.01$, and *** for $p < 0.001$.

Supplementary Material

Refer to Web version on PubMed Central for supplementary material.

Acknowledgments

The authors would like to thank Dr. Carolyn Lane (Valley View Family Practice Clinic, Calgary, AB, Canada) for providing foreskin specimens for isolation of primary dermal microvascular endothelial cells, Dr. Charles T. Esmon for helpful discussions, and the Live Cell Imaging Facility, Snyder Institute for Chronic Diseases, University of Calgary for the use of the confocal microscope. Funding for this work was provided by the Canadian Institutes of

Health Research grant MT14104 (M.H.) and by the National Institutes of Health grants R56 AI104238 and RO1 AI47953 (J.D.S.).

References

Avril M, Tripathi AK, Brazier AJ, Andisi C, Janes JH, Soma VL, et al. A restricted subset of var genes mediates adherence of *Plasmodium falciparum*-infected erythrocytes to brain endothelial cells. Proc Natl Acad Sci USA. 2012; 109:E1782–E1790. [PubMed: 22619321]

Avri, l M.; Brazier, AJ.; Melcher, M.; Sampath, S.; Smith, JD. DC8 and DC13 var genes associated with severe malaria bind avidly to diverse endothelial cells. PLoS Pathog. 2013; 9:e1003430. [PubMed: 23825944]

Bae J-S, Yang L, Manithody C, Rezaie AR. The ligand occupancy of endothelial protein C receptor switches protease-activated receptor1-dependent signaling specificity of thrombin from a permeability-enhancing to a barrier-protective response in endothelial cells. Blood. 2007; 110:3909–3916. [PubMed: 17823308]

Burnier L, Mosnier LO. Novel mechanisms for activated protein C cytoprotective activities involving noncanonical activation of protease-activated receptor 3. Blood. 2013; 122:807–816. [PubMed: 23788139]

Claessens A, Adams Y, Ghumra A, Lindergard G, Buchan CC, Andisi CC, et al. A subset of group A-like var genes encodes the malaria parasite ligands for binding to human brain endothelial cells. Proc Natl Acad Sci USA. 2012; 109:E1772–1781. [PubMed: 22619330]

Davis SP, Lee K, Gillrie MR, Rao L, Amrein M, Ho M. CD36 recruits $\alpha_5\beta$- integrin to promote cytoadherence of *P. falciparum*-infected erythrocytes. PLoS Pathog. 2013; 9:e1003590. 21. [PubMed: 24009511]

Dorovini-Zis K, Schmidt K, Huynh H, Fu W, Whitten RO, Milner DA, et al. The neuropathology of fatal cerebral malaria in Malawian children. Am J Pathol. 2011; 178:2146–2158. [PubMed: 21514429]

Finigan JH, Dudek SM, Singleton PA, Chiang ET, Jacobson JR, Camp SM, et al. Activated protein C mediates novel lung endothelial barrier enhancement: role of sphingosine 1-phosphate receptor transactivation. J Biol Chem. 2005; 280:17286–1729393. [PubMed: 15710622]

Francischetti IM, Seydel KB, Monteiro RQ, Whitten RO, Erexson CR, Noronha AL, et al. *Plasmodium falciparum*-infected erythrocytes induce tissue factor expression in endothelial cells and support the assembly of multimolecular coagulation complexes. J Thromb Haemost. 2007; 5:155–165. [PubMed: 17002660]

Gillrie MR, Krishnegowda G, Lee K, Buret AG, Robbins SM, Ho M. Src-family kinase dependent disruption of endothelial barrier function by *Plasmodium falciparum* merozoite proteins. Blood. 2007; 110:3426–3435. [PubMed: 17693580]

Ho M, Hickey MJ, Murray AG, Andonegui A, Kubes P. Visualization of *Plasmodium falciparum*-endothelium interactions in human microvasculature: mimicry of leukocyte recruitment. J Exp Med. 2000; 192:1205–1211. [PubMed: 11034611]

Janes JH, Wang CP, Levin-Edens E, Wigan-womas I, Guillotte M, Melcher M, et al. Investigating the host binding signature on the *Plasmodium falciparum* PfEMP1 protein family. PLoS Pathog. 2011; 7:e1002032. [PubMed: 21573138]

Lavstsen T, Turner L, Saguti F, Magistrado P, Rask TS, Jespersen JS, et al. *Plasmodium falciparum* erythrocyte membrane protein 1 domain cassettes 8 and 13 are associated with severe malaria in children. Proc Natl Acad Sci USA. 2012; 109:E1791–E1800. [PubMed: 22619319]

Laszik Z, Mitro A, Taylor FB, Ferrell G, Esmon CT. Human protein C receptor is present primarily on endothelium of large blood vessels: implications for the control of the protein C pathway. Circ. 1997; 96:3633–3640.

Lau CK, Turner L, Jespersen JS, Lowe ED, Petersen B, Wang CW, et al. Structural conservation despite huge sequence diversity allows EPCR binding by the PfEMP1 family implicated in severe childhood malaria. Cell Host Microbe. 2015; 17:1–12. [PubMed: 25590752]

Liaw PC, Mather T, Oganesyan N, Ferrell GL, Esmon CT. Identification of the protein C/activated protein C binding sites on the endothelial cell protein C receptor. Implications for a novel mode of

ligand recognition by a major histocompatibility complex class 1-type receptor. J Biol Chem. 2001; 276:8364–8370. [PubMed: 11099506]

MacPherson GG, Warrell MJ, White NJ, Looareesuwan S, Warrell DA. Human cerebral malaria. A quantitative ultrastructural analysis of parasitized erythrocyte sequestration. Am J Pathol. 1985; 119:385–401. [PubMed: 3893148]

McLaughlin JN, Patterson MM, Malik AB. Protease-activated receptor-3 (PAR3) regulates PAR1 signaling by receptor dimerization. Proc Natl Acad Sci USA. 2007; 104:5662–5667. [PubMed: 17376866]

Menschikowski M, Hagelgans A, Eisenhofer G, Siegert G. Regulation of endothelial protein C receptor shedding by cytokines is mediated through differential activation of MAP kinase signaling pathways. Exp Cell Res. 2009; 315:2673–2682. [PubMed: 19467228]

Mihara K, Ramachandran R, Renaux B, Salfeddine M, Hollenberg MD. Neutrophil elastase and proteinase-3 trigger G protein-biased signaling through proteinase-activated receptor-a (PAR1). J Biol Chem. 2013; 288:32979–32990. [PubMed: 24052258]

Milner DA, Factor R, Whitten R, Carr RA, Kamiza S, Pinkus G, et al. Pulmonary pathology in pediatric cerebral malaria. Human Pathol. 2013; 44:2719–2726. [PubMed: 24074535]

Milner DA, Whitten RO, Kamiza S, Carr RJ, Liomba G, Dzamalala C, et al. The systemic pathology of cerebral malaria in African children. Front Cell Infect Microbiol. 2014; 4:104. [PubMed: 25191643]

Mosnier L O, Zlokovic BV, Griffin JH. The cryoprotective protein C pathway. Blood. 2007; 109:3161–3172. [PubMed: 17110453]

Mosnier LO, Sinha RK, Burnier L, Bouwens EA, Griffin JH. Biased agonism of protease activated receptor 1 by activated protein C caused by noncannoical cleavage at Arg 46. Blood. 2013; 120:5237–5248. [PubMed: 23149848]

Moxon CA, Wassmer SC, Milner DA, Chisala NV, Taylor TE, Seydel KB, et al. Loss of endothelial protein C receptors links coagulation and inflammation to parasite sequestration in cerebral malaria in African children. Blood. 2013; 122:842–851. [PubMed: 23741007]

Rask TS, Hansen DA, Theander TG, Gorm Pedersen A, Lavstsen T. *Plasmodium falciparum* erythrocyte membrane protein 1 diversity in seven genomes-divide and conquer. PLoS Comput Biol. 2010; 6:e1000933. [PubMed: 20862303]

Robinson BA, Welch TL, Smith JD. Widespread functional specialization of *Plasmodium falciparum* erythrocyte membrane protein 1 family members to bind CD36 analysed across a parasite genome. Mol Microbiol. 2003; 47:1265–18. [PubMed: 12603733]

Rowe JA, Claessens A, Corrigan RA, Arman M. Adhesion of *Plasmodium falciparum*-infected erythrocytes to human cells: molecular mechanisms and therapeutic implications. Expert Rev Mol Med. 2009; 11:e16. [PubMed: 19467172]

Russo A, Soh UJK, Paing MM, Arora P, Trejo J. Caveolae are required for protease selective signaling by protease-activated receptor 1. Proc Natl Acad Sci USA. 2009; 106:6393–6397. [PubMed: 19332793]

Sen P, Sahoo S, Pendurthi UR, Rao LVM. Zinc modulates the interaction of protein C and activated protein C with endothelial cell protein C receptor. J Biol Chem. 2007; 285:20410–20420. [PubMed: 20413590]

Smith JD, Kyes S, Craig AG, Fagan T, Hudson-Taylor D, Miller LH, et al. Analysis of adhesive domains from the A4VAR *Plasmodium falciparum* erythrocyte membrane protein-1 identifies a CD36 binding domain. Mol Biochem Parasitol. 1998; 97:133–148. [PubMed: 9879893]

Stins MF, Badgera J, Kim KS. Bacterial invasion and transcytosis in transfected human brain microvascular endothelial cells. Micro Pathogen. 2001; 30:19–28.

Taylor TE, Fu WJ, Carr RJ, Whitten RO, Mueller JS, Fosiko NG, et al. Differentiating the pathologies of cerebral malaria by post-mortem parasite counts. Nat Med. 2004; 10:143–145. [PubMed: 14745442]

Tembo DL, Nyoni B, Murikoli RV, Mukaka M, Milner DA, Berriman M, et al. Differential PfEMP1 expression is associated with cerebral malaria pathology. PLoS Pathogens. 2014; 10:e1004537. [PubMed: 25473835]

Turner L, Lavstsen T, Berger SS, Wang CW, Petersen JE, Avril M, et al. Severe malaria is associated with parasite binding to endothelial protein C receptor. Nature. 2013; 498:502–505. [PubMed: 23739325]

White NJ, Turner GD, Day NP, Dondorp AM. Lethal malaria: Marchiafava and Bignami were right. J Infect Dis. 2013; 28:192–198. [PubMed: 23585685]

Yipp BG, Anand S, Schollaardt T, Patel KD, Looareesuwan S, Ho M, et al. Synergism of multiple adhesion molecules in mediating cytoadherence of *Plasmodium falciparum*-infected erythrocytes to microvascular endothelial cells under flow. Blood. 2000; 96:2292–2298. [PubMed: 10979979]

Yipp BG, Baruch DI, Brady C, Murray AG, Looareesuwan S, Kubes P, Ho M, et al. Recombinant PfEMP1 peptide inhibits and reverses cytoadherence of clinical *Plasmodium falciparum* isolates in vivo. Blood. 2003; 101:331–337. [PubMed: 12393525]

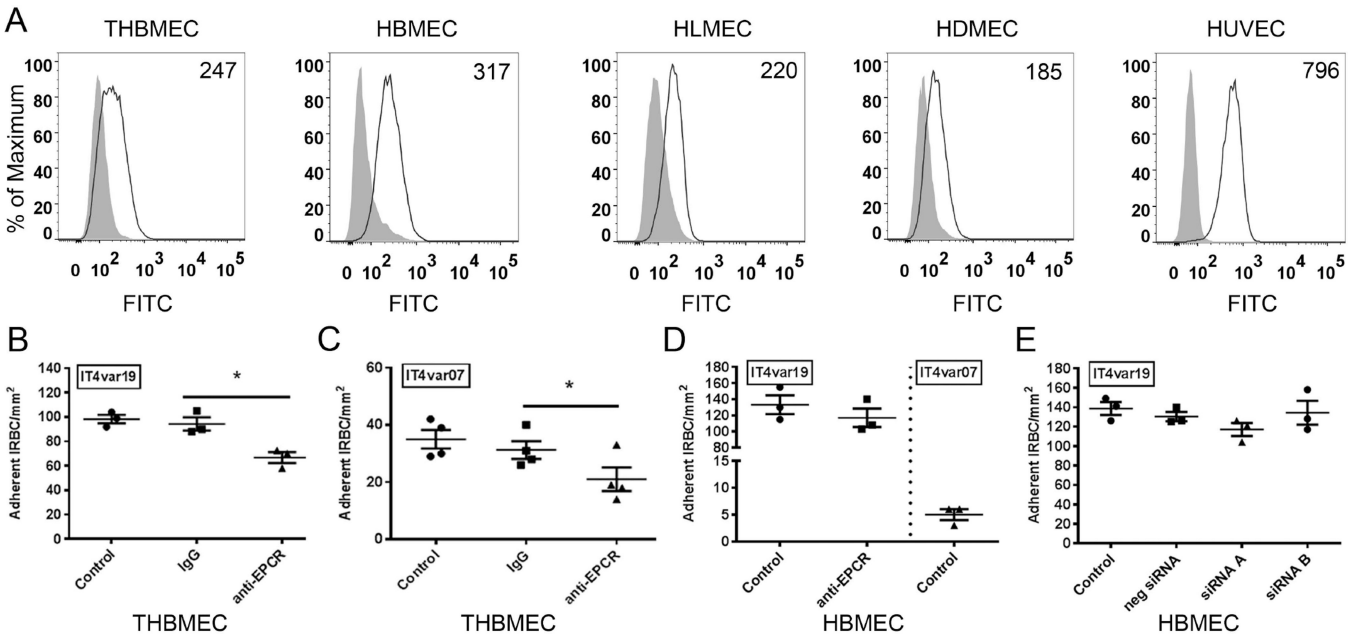

Figure 1. EPCR contributed to adhesion of DC8 and DC-13-expressing *P. falciparum* IRBC to THMEC but not HBMEC under shear stress

Adhesion assays were performed using IT4var19 and IT4var07 IRBC at 1% hematocrit and 4–5% parasitemia in a parallel-plate flow chamber at 1dyne/cm^2. (A) Flow cytometric analysis of EPCR surface expression on THBMEC, HBMEC, HLMEC, HDMEC and HUVEC. The MFI values for EPCR expression are given in the top right corner of each histogram. Results shown are representative of 3 experiments. (B) IT4var19 IRBC adhesion to THBMEC was partially inhibited by anti-EPCR (n-3). (C) IT4var07 IRBC adhesion to THBMEC was partially inhibited by anti-EPCR (n-3). (D) IT4var19 adhesion to HBMEC was not inhibited by anti-EPCR antibody (n=3). (E) Lack of effect of EPCR protein knock down on IT4var19 adhesion to HBMEC (n=3). Results were analyzed by ANOVA followed by post-hoc multiple comparisons using Tukey's test. *$p < 0.05$. n=number of independent experiments.

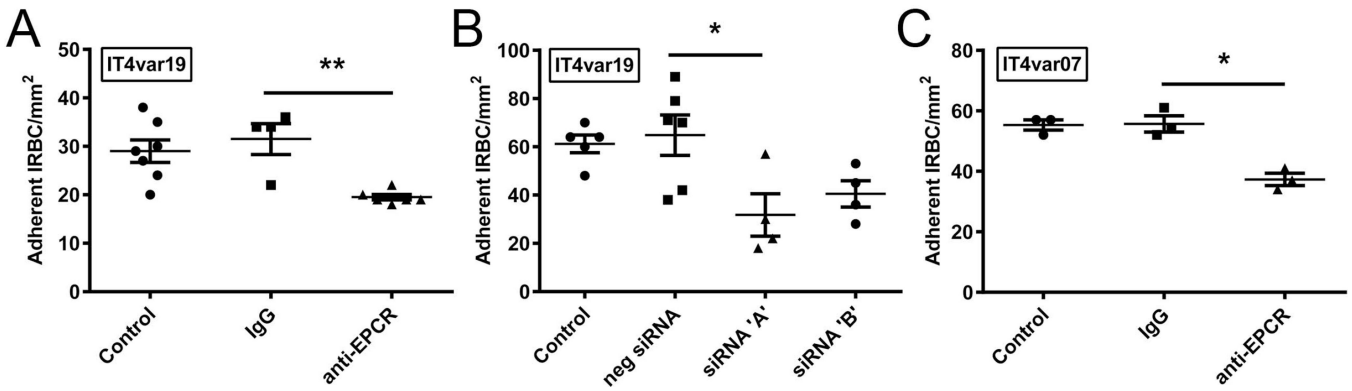

Figure 2. EPCR contributed to adhesion of DC8 and DC-13-expressing *P. falciparum* IRBC to HLMEC

(A) IT4var19 IRBC adhesion to HLMEC was partially inhibited by anti-EPCR (n = 7 for control, 4 for rat IgG and 7 for anti-EPCR). (B) Adhesion of IT4var19 IRBC to HLMEC was partially inhibited by knockdown of EPCR protein expression by 2 different siRNA (n=3). (C) Adhesion of IT4var07 IRBC to HLMEC was partially inhibited by anti-EPCR (n=3). Results were analyzed by ANOVA followed by post-hoc multiple comparisons using Tukey's test. *$p < 0.05$, **$p < 0.01$. n=number of independent experiments.

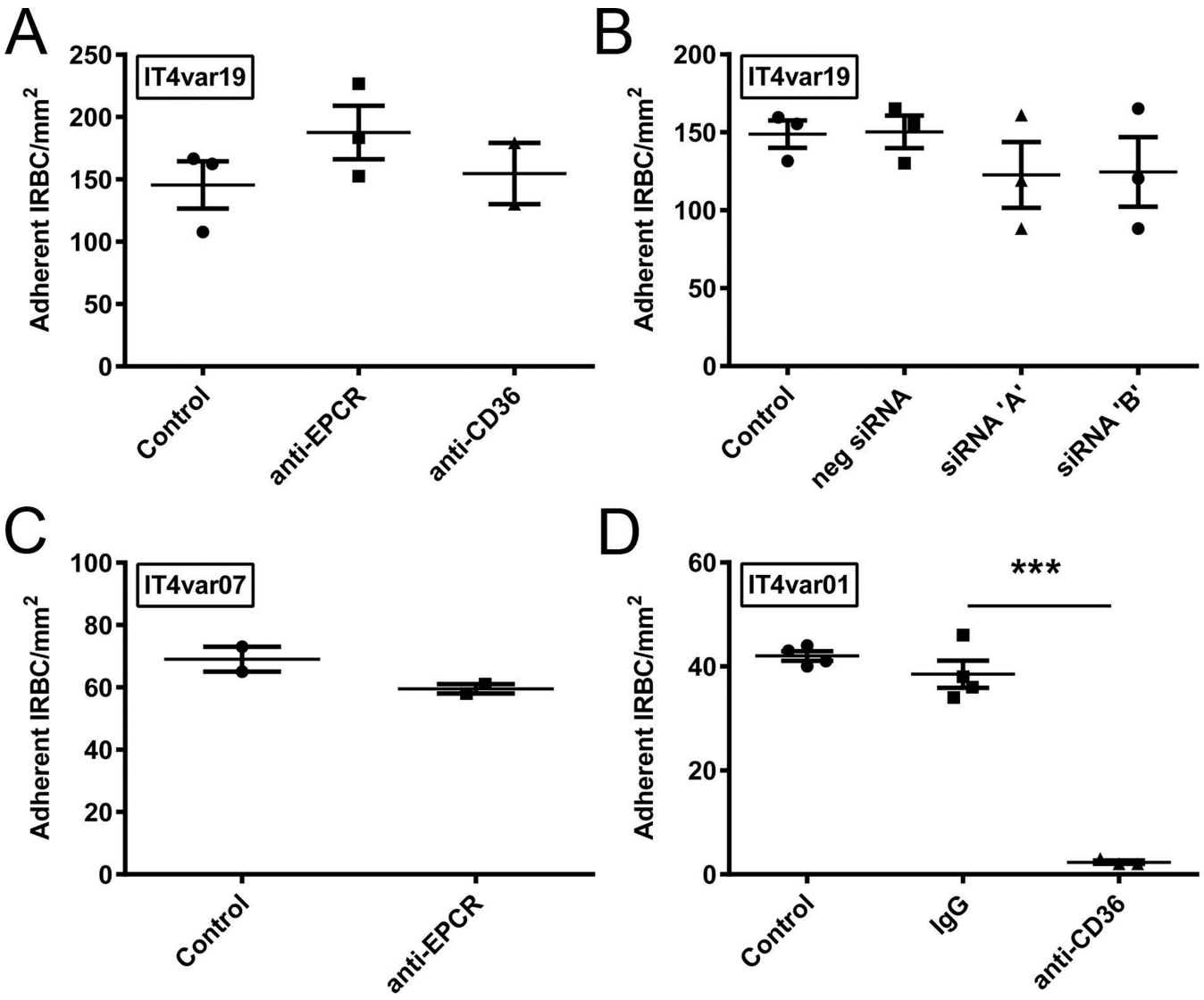

Figure 3. EPCR did not contribute to adhesion of DC8 and DC-13-expressing *P. falciparum* IRBC to HDMEC

(A) Adhesion of IT4var19 IRBC to HDMEC was not inhibited by anti-EPCR (n=3). (B) Adhesion of IT4var19 IRBC to HDMEC was not inhibited by siRNA knockdown of EPCR expression (n=4–7). (C) Adhesion of IT4var07 IRBC to HDMEC was not inhibited by anti-EPCR (n=2). (D) Adhesion of a control CD36-binding IT4var01 IRBC expressing CIDRα6 to HDMEC was completely inhibited by anti-CD36 (n=4). Results were analyzed by ANOVA followed by post-hoc multiple comparisons using Tukey's test. *** $p < 0.001$. n=number of independent experiments.

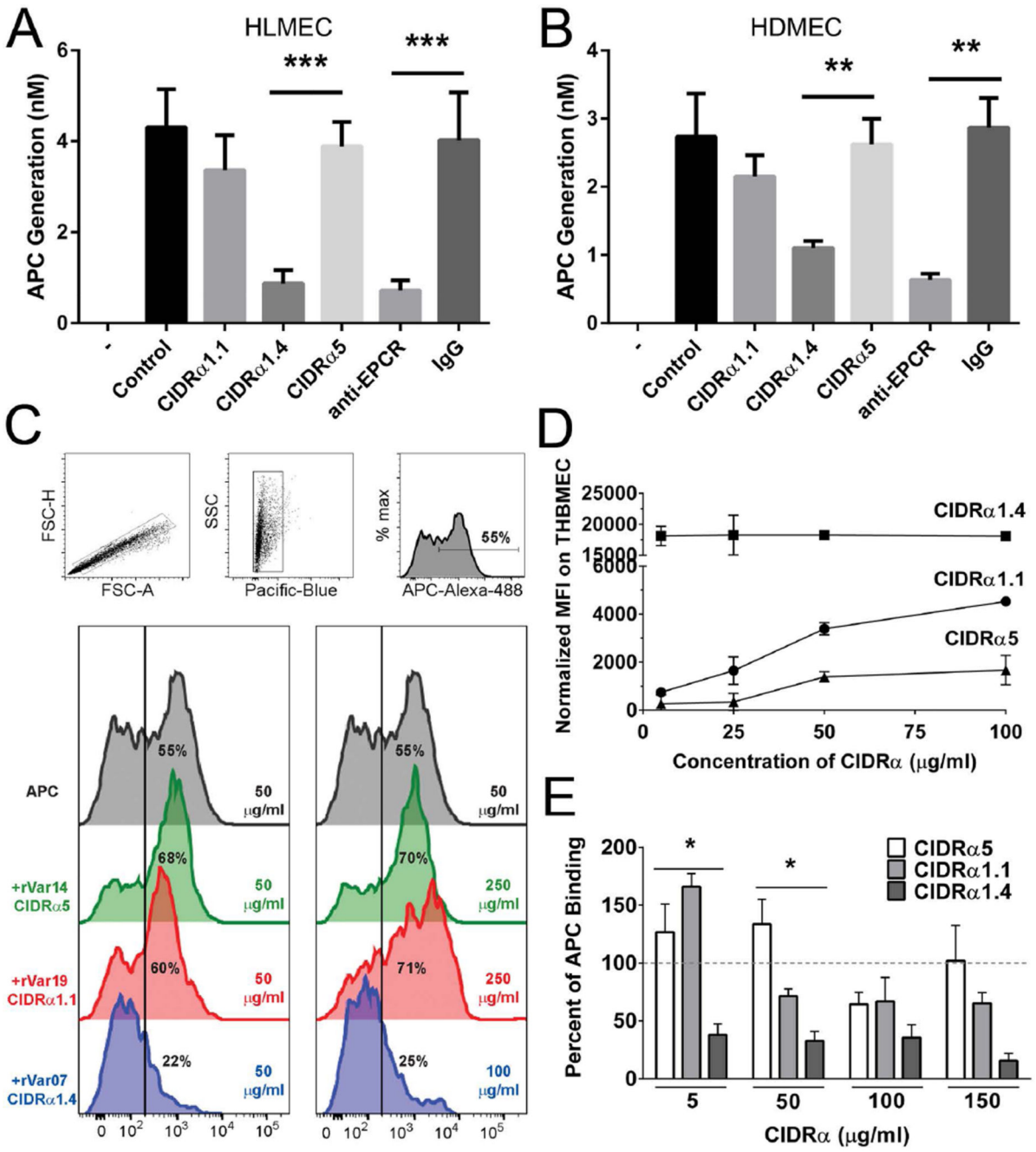

Figure 4. IT4var07 CIDRα1.4 but not IT4var19 CIDRα1.1 inhibited APC generation and binding of APC to endothelial cells

The amidolytic APC generation assay using the chromogenic substrate S-2366 was performed to determine the effect of CIDRα1.1- and CIDRα1.4-coated beads on EPCR-dependent APC generation from protein C and thrombin. (A) APC generation by HLMEC in the presence of CIDR-beads or anti-EPCR (20 µg/ml) (n=5). (B) APC generation by HDMEC in the presence of CIDR-beads or anti-EPCR (20 µg/ml) (n=4). (C) Stacked histograms showing APC binding when THBMEC were co-incubated with CIDR recombinant proteins and 50 µg/ml APC. Surface labeling of APC was detected via a

specific anti-APC antibody. The top histogram shows APC binding on its own. The stacked histograms show APC binding in the presence of a negative control CD36 binding domain (Var14 CIDRα5) or two different EPCR binding domains (var19 CIDRα1.1 and var07 CIDRα1.4). The gating strategy for panels C and E is shown at the top of panel C. Results shown are representative of two independent experiments. (D) Binding titration from 5 μg/ml to 100 μg/ml of three recombinant CIDR proteins on THBMEC as determined by flow cytometry. Results are expressed as mean normalized MFI relative to control (THBMEC in presence of primary and secondary antibodies alone) ± SD for n=2. (E) Inhibition of APC binding to THBMEC that were pre-incubated for 30 min with varying concentrations of CIDR recombinant proteins (5, 50, 100, 150 μg/ml) prior to adding APC at 50 μg/ml. APC binding was detected via a specific anti-APC antibody (n=2–6). Results shown were analyzed using ANOVA followed by post-hoc multiple comparisons using Tukey's test. * $p < 0.05$, ** $p < 0.01$, *** $p < 0.001$. n=number of independent experiments.

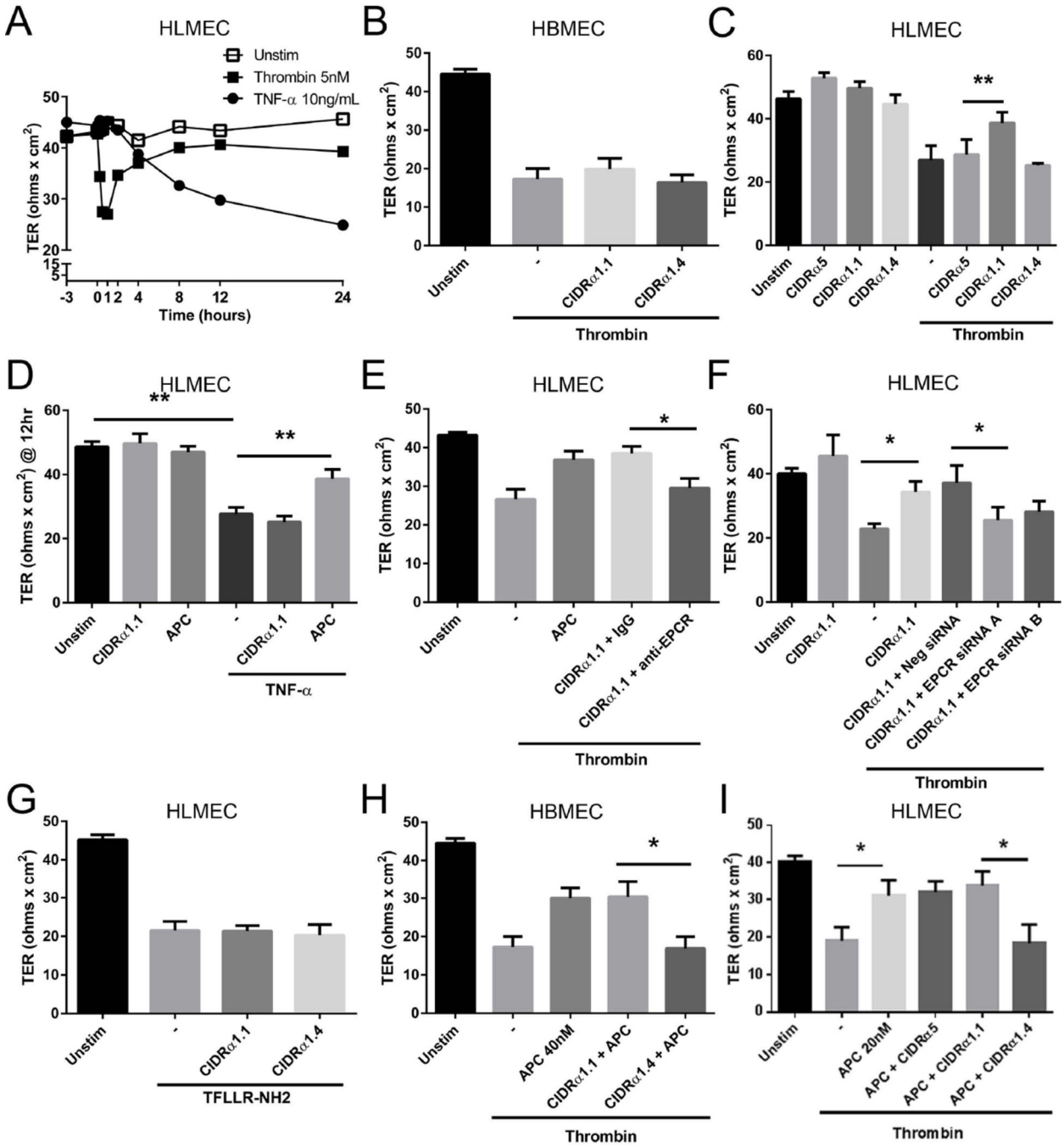

Figure 5. IT4var19 CIDRα1.1 but not IT4var07 CIDRα1.4 domains inhibited endothelial barrier dysfunction induced by thrombin

Transwell permeability assays were performed with 3-day post-confluent HBMEC and HLMEC monolayers using serial trans-endothelial resistance (TER) readings as a measure of permeability. (A) Representative time course of TER for HLMEC treated with TNF-α (10ng/mL) or thrombin (5nM) over 24 hours. (B) IT4var19 CIDRα1.1- and IT4var07 CIDRα1.4-beads had no effect on thrombin-induced permeability on HBMEC (n=4). (C) CIDRα1.1- but not CIDRα1.4-beads partially inhibited thrombin-induced permeability on HLMEC (n=6). (D) Lack of effect of CIDRα1.1-beads on TNF-α induced permeability at

12h (n=3). (E) Blockade of EPCR by anti-EPCR (20μg/mL) reduced the protective effect of CIDRα1.1-beads on thrombin-induced barrier dysfunction (n=3). (F) Knock down of EPCR by siRNA 'A' and 'B' inhibited the protective effect of CIDRα1.1-beads on thrombin-induced barrier dysfunction (n=3). (G) Lack of effect of CIDRα1.1-beads on permeability induced by the PAR-1 agonist peptide TFLLR-NH2 (20μM) (n=3). (H) CIDRα1.4-beads inhibited the barrier protective effect of APC (40nM) on thrombin (10nM)-induced permeability in HBMEC (n=4). (I) CIDRα1.4- and not CIDRα1.1-beads inhibited the barrier protective effect of APC (20nM) on thrombin (5nM)-induced permeability in HLMEC (n=4). With the exception of panels (A) and (D), all panels display TER values from the 30 min time point at which the effect of thrombin or TFLLR-NH2 on TER was maximal. Results shown were analyzed using ANOVA followed by post-hoc multiple comparisons using Tukey's test. *$p < 0.05$, ** $p < 0.01$, *** $p < 0.001$. n=number of independent experiments.

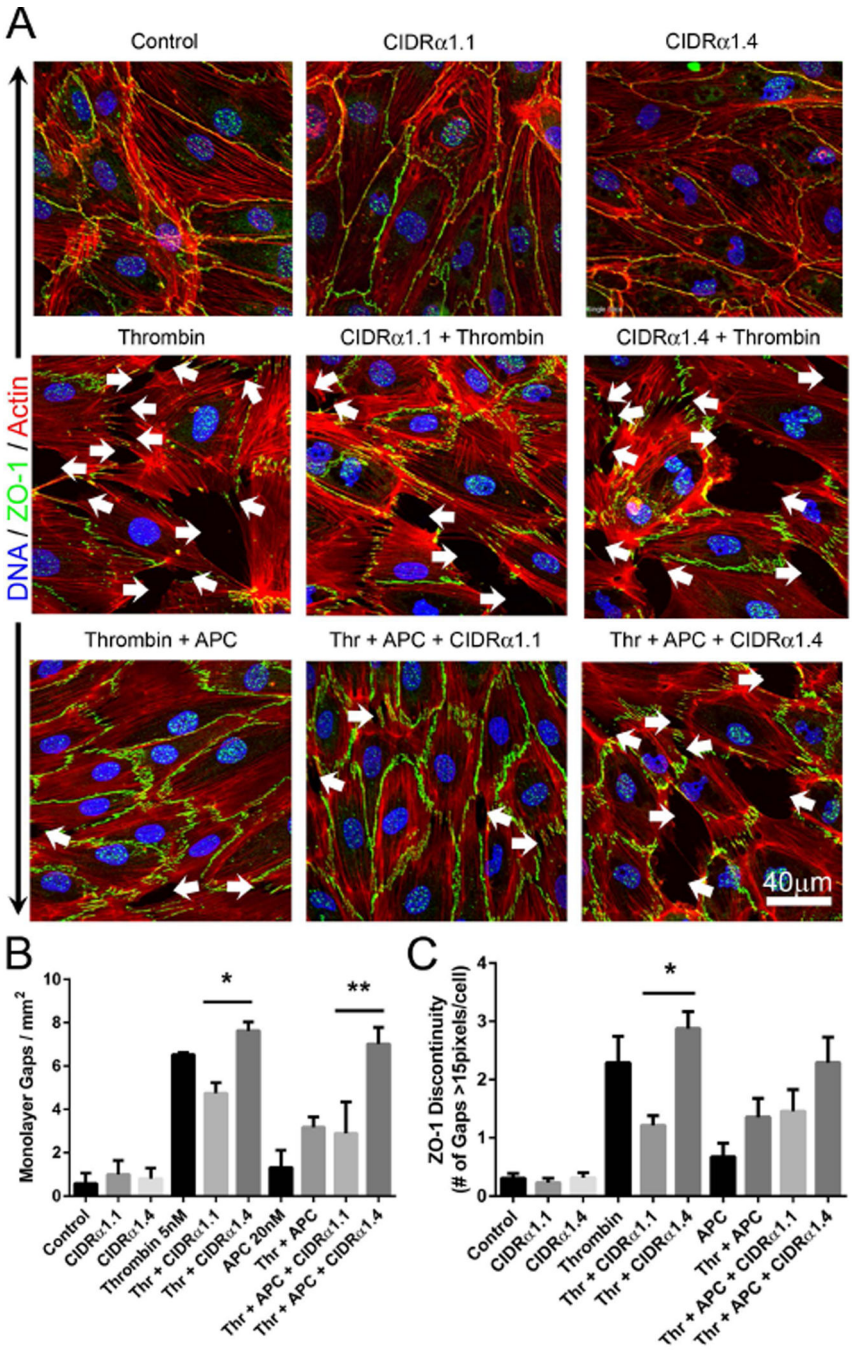

Figure 6. IT4var19 CIDRα1.1 but not IT4var07 CIDRα1.4 inhibited thrombin- induced gap formation and ZO-1 discontinuity in HLMEC

Post-confluent HLMEC in ibidi VI chambers were pre-incubated with CIDRα1.1- or CIDRα1.4-beads ($2.5\times10^6/cm^2$) for 30 min, followed by either APC (20nM) or buffer for 30 min and then thrombin (5nM) for 30 min at 37°C in 5% CO_2. The monolayers were washed 2x with HBSS to remove unbound beads prior to fixing with 1% PFA for 30 min at room temperature. Fixed cells were stained with a rabbit polyclonal antibody against ZO-1, followed by Alexa 488-labeled goat anti-rabbit IgG, rhodamine phalloidin for actin and Hoechst 33342 for DNA. All images were taken on an Olympus IX81 inverted confocal

microscope (Center Valley, Pa) with Fluorview 1000 acquisition software using a PlanAPO 40X N.A. 1.43 objective. (A) Junctional protein (ZO-1) disruption and intercellular gap formation (indicated by white arrows) induced by thrombin was partially reversed by pre-incubation with CIDRα1.1- but not CIDRα1.4-beads. In contrast, CIDRα1.4- but not CIDRα1.1-beads abrogated the protective effect of APC. Images shown are representative of 3 independent experiments for each condition. (B) and (C) Quantification of microscopic changes seen in (A). For every condition in every experiment, three randomly selected microscopic fields at 40X magnification were examined. (B) Number of intercellular gaps of >20 pixels in diameter. (C) Discontinuity in ZO-1 staining of >15pixels in length at sites of cell-cell junctions (C). Results were analyzed using ANOVA followed by post-hoc multiple comparisons using Tukey's test. * $p < 0.05$, ** $p < 0.01$, *** $p < 0.001$.

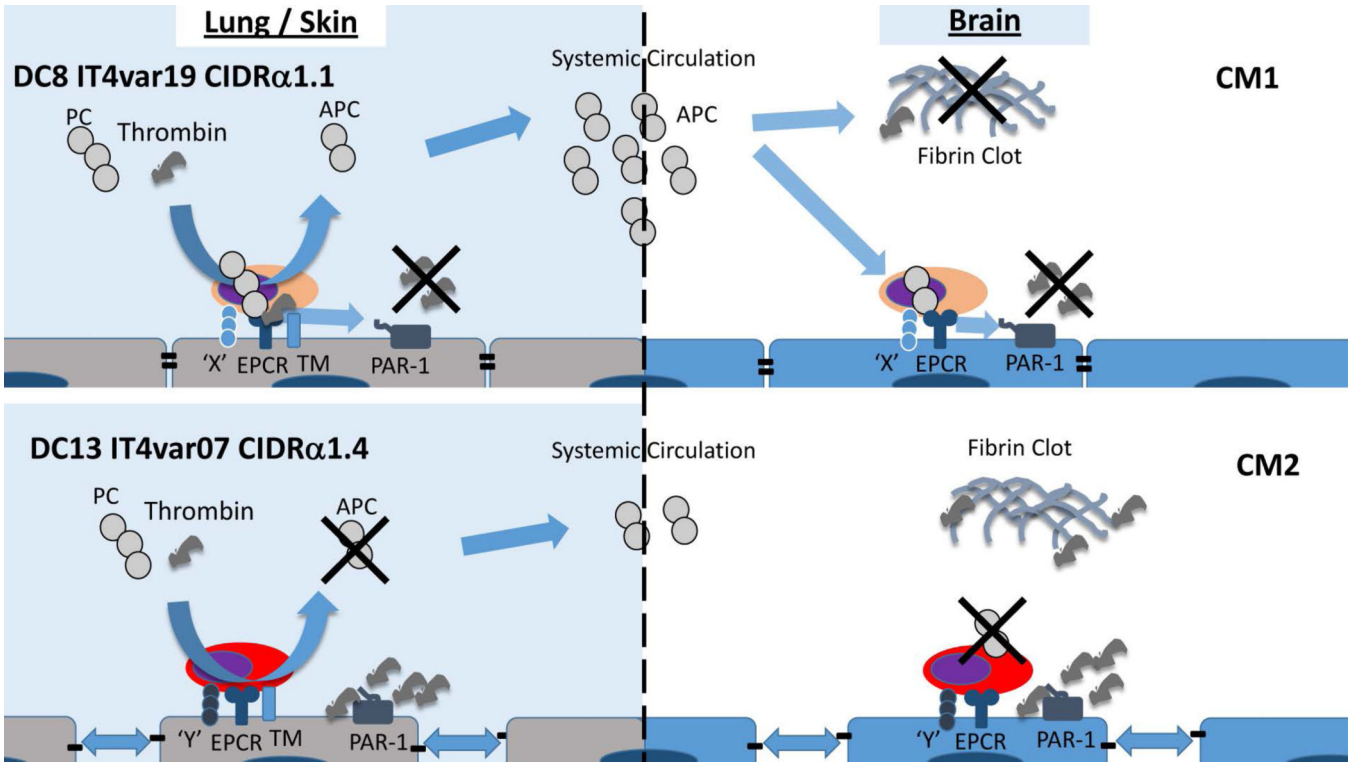

Figure 7. Proposed model for the divergent effects of DC8 and DC13 CIDRα1 engagement of EPCR in different organs

(Top panel) DC8 CIDRα1.1 expressing parasites adhere to lung, dermal and brain microvascular endothelium under shear stress with differential requirement for EPCR and as yet unidentified receptors (X). Adhesion of these parasites in the lung and skin does not interfere with endothelial APC generation. The brain microvasculature does not support APC generation locally (due to low or absent thrombomodulin expression) but can respond to systemically released APC in the presence of CIDRα1.1-expressing parasites. In addition, EPCR engagement by CIDRα1.1-type parasites may shift thrombin signaling from barrier disruptive to barrier protective pathways. As a result, DC8 CIDRα1.1 parasite adhesion to EPCR may lead to dense sequestration of IRBC with relatively little evidence of coagulopathy. These pathological features are compatible with those described in the CM1 subtype of cerebral malaria. (Bottom panel) DC13 CIDRα1.4 parasites also adhere to different types of microvascular endothelial cells under flow conditions, but the adhesion is only partially dependent on EPCR and requires additional receptors (Y). In contrast to DC8 CIDRα1.1, DC13 CIDRα1.4 expressing parasites strongly inhibit APC generation and APC binding to EPCR and hence abrogate the protective effect of APC in diverse vascular beds including the brain. Pathologically this could be represented by the diffuse fibrin clots in the brain, lung and kidney in addition to more widespread inflammation seen in the CM2 subtype of cerebral malaria. The functional dichotomy of IT4var19 CIDRα1.1 and IT4var07 CIDRα1.4 may be related to differential binding characteristics of the proteins on EPCR.